

Novel Joining of Dissimilar Ceramics in the $\text{Si}_3\text{N}_4\text{-Al}_2\text{O}_3$ System Using Polytypoid Functional Gradients

Caroline S. Lee^{1,2}, Xiao Feng Zhang¹ and Gareth Thomas^{1,2}

1. Materials Science Division

Lawrence Berkeley National Laboratory, Berkeley, CA 94720

and

2. Department of Materials Science and Mineral Engineering,

University of California, Berkeley, CA 94720

ABSTRACT

A unique approach to crack-free joining of heterogeneous ceramics is demonstrated by the use of sialon polytypoids as Functionally Graded Materials (FGM) as defined by the phase diagram in the system, $\text{Si}_3\text{N}_4\text{-Al}_2\text{O}_3$. Polytypoids in the $\text{Al}_2\text{O}_3\text{-Si}_3\text{N}_4$ system offer a path to compatibility for heterogeneous ceramics. This paper describes successful hot press sintering of multilayered FGM's with 20 layers of thickness 500 μm each.

Transmission Electron Microscopy was used to identify the polytypoids at the interfaces of different areas of the joint. It has been found that the 15R polytypoid was formed in the Al_2O_3 -contained layers and the 12H polytypoid was formed in the Si_3N_4 -contained layers.

Keywords: Functionally Graded Materials (FGM), Sialon polytypoids, Si_3N_4 , Al_2O_3 , and High-resolution electron microscopy

1. INTRODUCTION

The joining of materials is an important process commercially and technologically. Due to the existence of physical and economic limitations for the manufacture of large parts, joining is essential. Further, for fabrication of complex shapes, it is much easier to make regular geometric shapes and then join them. Finally, having different materials at different regions of the same component is desirable for several applications [1]. Joining to form these components is often the only way for fabrication.

Gopal et al. [2,3], have performed experiments on the joining of Si_3N_4 to itself, using a rare-earth silicate glass which is a ceramic interlayer, following earlier work on sintering Si_3N_4 to produce glass free joints [4, 5]. However, these interlayers cannot be used to join dissimilar materials. This is because of the large difference in their coefficients of thermal expansion, which leads to the development of stresses, which cause failure. The joining of these different materials can be effected using Functionally Graded Materials (FGMs). In an FGM, there is a continuous change in composition from one region to another. When an FGM is used, the shrinkage is dependent on the concentration of the species present locally. The FGM can therefore accommodate the shrinkage strain and join with dissimilar materials. In this work, polytypoidal functional gradients have been used to join the dissimilar ceramics, Si_3N_4 and Al_2O_3 .

Silicon nitride has been considered as one of the most promising structural materials for high temperature applications for the following unique properties - high strength, oxidation and corrosion resistance, thermal stability and resistance to thermal shock [6]. Alumina has been chosen for the joining material since it has an intermediate

coefficient of thermal expansion between Si_3N_4 and metals. Alumina can be used as a buffer layer for joining Si_3N_4 and metal. Moreover, it has been widely used in high temperature structural components due to its chemical stability.

In order to join Si_3N_4 to Al_2O_3 , a sialon polytypoid has been used for several reasons; first, sialons are essentially silicates and alumino-silicates in which oxygen is partly or completely replaced by nitrogen, while silicon is partly replaced by aluminum [6]. Sialon polytypoids are physically and chemically compatible with both Si_3N_4 and Al_2O_3 . Because metal-nitrogen bonding is in general more covalent than metal-oxygen, there is freedom to vary the covalent: ionic contributions to the interatomic bonding in a variety of structures [7]. The relationships between Si-Al-O-N condensed phases are represented by the quaternary phase diagram (Figure 1) and any point in the square diagram Si_3N_4 - Al_4O_6 - Al_4N_4 - Si_3O_6 represents a combination of 12^+ and 12^- valences where the components adopt their usual valency states, (that is Si^{4+} , Al^{3+} , N^{3-} and O^{2-}). A polytypoid is defined as a faulted structure in which the fault periodicity depends on composition through the cation/anion ratio. These polytypoids are different from a polytype, which has a faulted structure with no change in composition, such as SiC. It was found that AlN polytypoids, such as 15R, 12H, 21R, 27R and 2H, have CTEs in the range of 5.1 to $5.9 \times 10^{-6} / ^\circ\text{C}$ [8]. Since the CTE of Si_3N_4 is $3.6 \times 10^{-6} / ^\circ\text{C}$ and that of Al_2O_3 is $8.8 \times 10^{-6} / ^\circ\text{C}$, the use of sialon polytypoids for joining Si_3N_4 and Al_2O_3 , is clearly attractive.

In this Si_3N_4 - Al_2O_3 system, there are six polytypoid phases from the sialon compositions between β' and AlN as shown in Figure 1. They have structures based on the AlN wurtzite-type (Figure 2). These phases are members of a new series of

polytypoids in which the structure is determined by the metal: nonmetal atom ratio M/X . The polytypoids have compositions M_mX_{m+1} where m is an integer 4 to 9 and the structures are described by the Ramsdell symbols 8H, 15R, 12H, 21R, 27R and 2H [6,7,9]. From Figure 2, the metal atoms (Al) form a hexagonal close-packed arrangement and the non-metal atoms (N) fill one-half of the available tetrahedral sites giving rise to the composition AlN. For AlN-rich compositions of the sialon system, the excess non-metal atoms are taken up by creating periodic stacking faults in the metal configuration and filling up a double layer of tetrahedra at every fault [9,10]. It is clear that the further the M/X ratio deviates from 1, the smaller is the stacking fault spacing. Therefore, polytypoid step functional joining can be obtained since the structure of this compound is determined by stacking-fault spacing (metal/non metal ratio) as explained above.

Another advantage of using a polytypoid as a functional gradient to join Si_3N_4 and Al_2O_3 is that polytypoids have mostly glass-free interfaces [9]. This is an essential property since elevated temperature strength is influenced by the presence of glassy phases at interfaces, notably grain boundaries, and triple junctions.

2. EXPERIMENTAL PROCEDURE

(1) Material Fabrication

To create FGMs, a "mixture rule" was applied to make the gradient since it has been widely used in the modeling of FGMs [11,12]. A material having two components, denoted as A and B, is considered. Let P_A and P_B be the values of some particular property for pure A and pure B, respectively, and let their respective volume fractions be f_A and f_B , where $f_B = 1 - f_A$ assuming that the material is 100% dense. For an

FGM, these values of f are dependent upon position along the graded direction. The well-known Voigt-type estimate for the effective value, P , of the property of FGM is

$$P = f_A P_A + f_B P_B$$

This "mixture rule" was applied to calculate Coefficient of Thermal Expansion (CTE) of each graded layer so that CTE difference of approximately $0.2 \times 10^{-6} / ^\circ\text{C}$ between each layer, would exist to minimize residual stress (Figure 3).

FGMs can be fabricated by a number of methods, such as powder processing [13], thermal spraying [14], CVD[15] and combustion synthesis [16], etc. For the experiment, powder processing was used to provide a wide range of compositional and microstructural control. Powder blending was done by wet milling of powders using Isopropanol as solvent. For powder processing, 6wt% Y_2O_3 and 2wt% Al_2O_3 were added as sintering additives to sinter Si_3N_4 . Si_3N_4 powders from H.C. Starck with a particle size ranging from 0.4 - 1.2 μm , were used, and Al_2O_3 powders from Sumitomo industries with the particle size ranging from 0.1 to 0.3 μm , were used. 12H sialon polytypoid powders were obtained from Novel Technologies. 3 wt.% Y_2O_3 was used as sintering additive for polytypoid powders.

Therefore, the FGM was fabricated by the following method; first, powders of each composition were mixed in isopropanol solvent, and then powders were agitated using the Ultrasonicator to prevent an agglomeration. These powders were dried, and sieved and were stacked layer by layer. The green body was pressed using a cold press to maintain a cylindrical shape. Finally, this green body was sintered using a Hot Press at 1700 $^\circ\text{C}$ for 2 hours in flowing N_2 gas to prevent decomposition of Si_3N_4 . A heating rate of 10 $^\circ\text{C}$ per minute was used to heat up to 1700 $^\circ\text{C}$ and hot pressing was used to achieve

full density. Following the densification, the sample was cooled with a cooling rate of 2 °C/min to minimize thermal stress build-up. Actual bulk densities were determined by the Archimedes method of weighing the sample in air and then in water, which was used as the immersion liquid.

(2) Microstructural Characterization

X-Ray Diffraction (XRD) was used to identify the phases present in the 100% polytypoid sample. To identify different polytypoids at various interfaces, high-resolution electron microscopy and electron diffraction were used since polytypoid has a distinct interplanar spacing. Also, high resolution images of grain boundaries were taken to identify grain boundary structure.

The specimens for Transmission Electron Microscopy (TEM) were prepared using conventional dimpling and ion milling methods. The sample pieces were cut to a thickness of about 250 µm. From this, a 3mm disc was cut out using an ultrasonic drill. The discs were then grounded to a thickness of 100 µm using a flattening tool. A dimple grinder was then used to form a dimple, with a 5-10 µm thin region in the middle. At this stage, the specimen is translucent to optical light. The specimens were then ion-milled, coated with a thin layer of carbon and analyzed in Philips CM200 transmission electron microscope working at 200 kV.

3. RESULTS AND DISCUSSION

(1) Crack-free joint

Direct joining of Si₃N₄-polytypoid-Al₂O₃ was tried at first to study if residual stress build-up among layers can be minimized by using a polytypoid interlayer, which

has an intermediate CTE between those of Si_3N_4 and Al_2O_3 . As shown in Figure 4a, cracks were developed due to residual stress build-up among the layers. In order to minimize residual stress, an FGM joint which consists of 20 graded layers, was introduced by a powder stacking method (Figure 4b). The composition along the gradient was varied by 10wt% to create a smooth gradient across the thickness. Previous studies have indicated that a better result can be obtained by varying the number of layers and the incremental change in composition from layer to layer, than by increasing the overall graded joint thickness [17]. Thus 20 layers were added to minimize the CTE mismatch stresses as much as possible (Figure 3). The density of this FGM sample using Archimedes method, was measured to be 96-97%. As can be seen from Figure 4b, the composite Si_3N_4 -polytypoids- Al_2O_3 is crack-free.

The sintering mechanism of this FGM is mostly liquid phase sintering as the process is essentially that of solution-precipitation within a eutectic liquid with accompanying particle rearrangement and phase transformation. Studies have shown that the alloying approach of Si_3N_4 and sialons to control the residual liquid content has been remarkably successful in producing an essentially single phase ceramic with outstanding high temperature mechanical properties. Although the sintering mechanism remains that of solution-precipitation, the liquid is transient and its components are largely removed by the solid solution such that grain boundaries contain only segregated ions within a width of the same order as the β' lattice spacing [18]. Nevertheless glassy phases may still be retained especially at triple junctions, but these may be crystallized in the presence of certain rare-earth additions. [2]

(2) Microstructural Characterization

An X-ray diffractometer was used to identify the phases present in the polytypoid powders before the FGM was fabricated (Figure 5). The polytypoids, $\text{Si}_3\text{Al}_7\text{O}_3\text{N}_9$ and $\text{Al}_5\text{Y}_3\text{O}_{12}$ were identified. The 001 d-spacing for $\text{Si}_3\text{Al}_7\text{O}_3\text{N}_9$ was found to be 2.7350 Å, which matches the published d-spacing value for the 12H polytypoid which is 2.74 Å. $\text{Al}_5\text{Y}_3\text{O}_{12}$ was formed in addition to the polytypoid due to the Y_2O_3 used as a sintering additive. Thus in the initial stages of sintering, Y_2O_3 forms yttrium aluminates through a solid state reaction with the oxygen-containing phase on the AlN powder surface, which accelerates sintering [19]. No undesirable reaction took place between Si_3N_4 and sialon polytypoid, and between Al_2O_3 and sialon polytypoid, as this observation agrees with the phase diagram (Figure 2).

High-resolution transmission electron microscopy was used to identify the polytypoid phases at various interfaces of the FGM, following earlier procedures [9,10]. For the areas in the Si_3N_4 -polytypoid area, the 12H polytypoid was identified ($c= 32.91$ Å). So the polytypoid did not change in the Si_3N_4 -polytypoid gradient area. However, in the Al_2O_3 -polytypoid gradient area, the polytypoid changed to 15R, $c= 41.81$ Å (Figure 6). This agrees with the trend of the phase diagram in Figure 1 where the polytypoid was transformed close to the materials to be joined, the closest polytypoid to Al_2O_3 is 15R and the one to Si_3N_4 is 12H. Thus the lattice mismatch is accommodated by having this polytypoid transformation closest to the materials being joined. Moreover, this trend in the polytypoid transformation from 12H to 15R as the ratio of cation to anion decreases, is exactly as predicted from the phase diagram (Figure 1). Thus the present approach can be applied to a wide range of ceramic systems including the superconductors [20].

High-resolution images were used to detect any glassy phases presented in grain boundaries since thermal stability is crucial for high temperature application. Various grain boundaries, such as $\text{Si}_3\text{N}_4/12\text{H}$, $15\text{R}/15\text{R}$, $12\text{H}/12\text{H}$ and $15\text{R}/\text{Al}_2\text{O}_3$, were imaged but no intergranular glassy phases were detected (Figures 7 a, b, c and d). However, statistically, one cannot exclude the existence of intergranular glassy phases in this polytypoid. For example, mechanical tests on these FGM samples implied that some glassy phases in the triple junction are present to cause strength degradation at high temperature [21].

5. CONCLUSIONS

(1) Crack-free joining of Si_3N_4 to Al_2O_3 (Figure 4b) was produced by stacking 20 layers of polytypoids with thickness of 500 μm each, to minimize thermal residual stress. The result showed a smooth gradient across the thickness with varying the composition along the gradient by 10 wt%. This method can be applied to other dissimilar ceramics as long as there is no undesirable reaction between the systems. In order to accomplish such processing effectively, accurate phase diagrams for each multicomponent system is needed.

(2) Microstructural characterization indicated that the 15R polytypoid was formed in the Al_2O_3 -contained layers and the 12H polytypoid was formed in the Si_3N_4 -contained layers. This transition in polytypoid from 12H to 15R is explained by phase diagram in Figure 1 where the closest polytypoid type is matched to the materials to be joined to accommodate the lattice mismatch, changing in polytypoid cation to anion ratios.

(3) No glassy phases were found across the various phases, such as $\text{Si}_3\text{N}_4/12\text{H}$, $15\text{R}/15\text{R}$, $12\text{H}/12\text{H}$ and $15\text{R}/\text{Al}_2\text{O}_3$.

6. ACKNOWLEDGEMENT

This work was supported by the Director, Office of Basic Energy Sciences, Division of Materials Sciences of the United States Department of Energy. The authors would like to thank Professor Lutgard C. DeJonghe for his support.

7. REFERENCES

1. M.M.Schwartz, "Ceramic Joining", ASM International (1990)
2. M. Gopal, L.C. DeJonghe and G. Thomas, "Silicon Nitride joining using rare-earth reaction sintering", *Scripta Materialia*, **36** (4), 455-460 (1997)
3. M. Gopal, L.C. DeJonghe and G. Thomas, "Silicon Nitride:From Sintering to joining", *Acta Mater.*, **46** (7), 2401-2405 (1998)
4. M.Cinbulk and G. Thomas, "Fabrication and secondary phase crystallization of Rare earth disilicate-silicon nitride ceramics", *Journal of American Ceramic Society*, **75** (no.8), 2037 (1992)
5. Y.Goto and G.Thomas, "Microstructure of silicon nitride ceramics sintered with rare earth oxides", *Acta metall. mater.*, **43**(no.3), 923 (1995)
6. P.M. Johnson and A. Hendry, "The microstructure of hot-pressed sialon polytypes", *Journal of Materials science* **14**, 2439 (1979)
7. K.H.Jack "The sialons", *Mat. Res. Bull.* **13**, 1327 (1978)
8. I. Yamai and T. Ota, "Thermal expansion of Sialon", *Advanced ceramic materials*, **2**(4), 784 (1987)
9. G.Van Tendeloo, K.T. Faber and G.Thomas, "Characterization of AlN cermaics containing long-period polytypes", *Journal of materials science*, **18**, 525 (1983)
10. K. H. Jack, "Review: Sialons and related nitrogen ceramics", *Journal of materials science* **11**, 1135 (1976)
11. A.J. Markworth, K.S. Ramesh and W. P. Parks Jr., "Review: Modelling studies applied to functionally graded materials", *Journal of Materials science*, **30**, 2183-2193 (1995)
12. Z. Fan, P. Tsakiroopoulos and A. P. Miodownik, "A generalized law of mixtures", *Journal of materials science*, **29**, 141-150 (1994)
13. R.Watanabe, "Powder processing of functionally gradient materials", *MRS Bulletin*, January, 32-34 (1995)
14. S. Sampath, H. Herma, N.Shimoda and T. Saito, "Thermal spray processing of FGMs", *MRS Bull.* **20**[1], 27 (1995)
15. T. Hirai, "CVD Processing", *MRS Bull.*, **20**[1], 45 (1995)

16. G.C. Stangle and Y. Miyamoto, "FGM fabrication by combustion synthesis", *MRS Bull.*, **20**[1], 52 (1995)
17. R.W. Messler, M. Jou and T.T. Orling, "A model for designing functionally gradient material joints", *Welding Journal*, **74**[5], S166 (1995)
18. M.H. Lewis and R.J. Lumby, "Nitrogen ceramics: liquid phase sintering", *Powder metallurgy*, **26**[2], 73-81 (1983)
19. N. Hashimoto and H. Yoden, "Sintering behavior of fine Aluminum Nitride powder synthesized from Aluminum polynuclear complexes" *Journal of American Ceramic Society*, **75** [8], 2098-106 (1992)
20. R.Ramesh, S. Green, C.Jiang, Y.Mei, M.Rudee, H.Luo and G. Thomas, "Polytypoid structure of Pb-modified Bi-Ca-Sr-Cu-O superconductor" *Physical Review B*, **38** [10], 7070-7073 (1988)
21. C. Lee, L.C. DeJonghe and G. Thomas, "Mechanical properties of Polytypoidally joined $\text{Si}_3\text{N}_4\text{-Al}_2\text{O}_3$ system" submitted to *Acta Mater.*

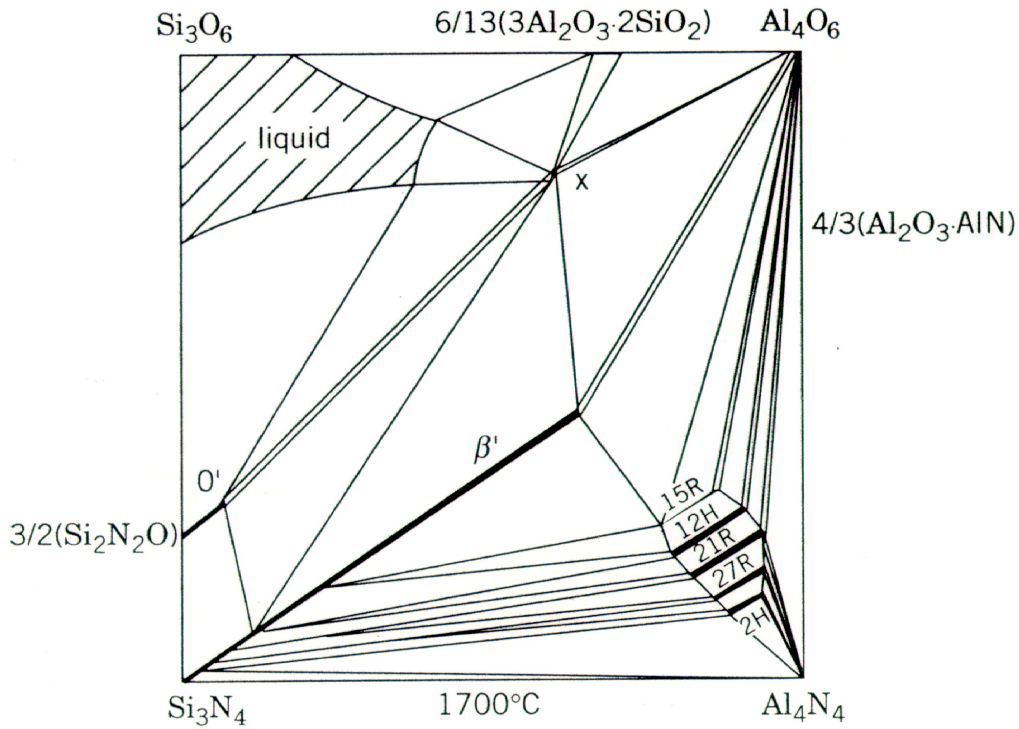


Figure 1. The Si-Al-O-N system (1700 °C) (Ref. K.H.Jack, Mat. Res. Soc. Sym. Proc., 1992, 287, p.16)

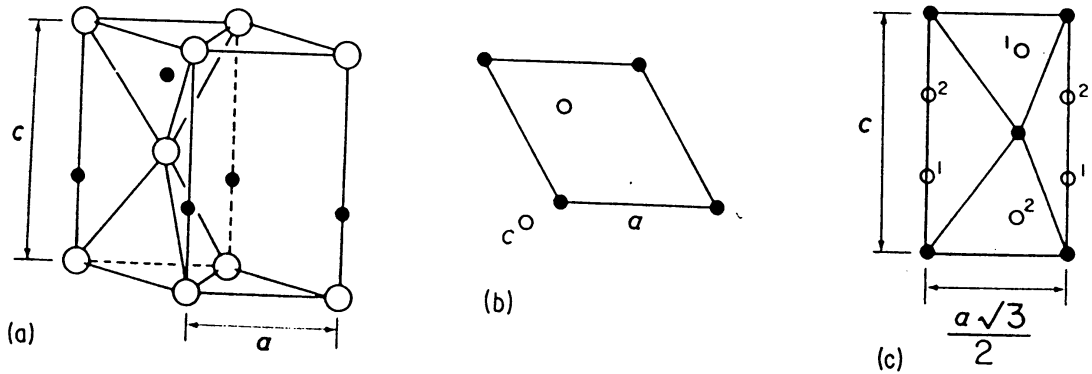


Figure 2. (a) Spatial view of the basic 2H wurzite structure. Metal atoms are represented by large open circles; anions are represented as small closed circles (b) Projection of the 2H structure along $[0\ 0\ 1]$; the non-metal atoms project along the metal atom configuration (c) Projection of 2H along $[1\ 0\ 0]$. The centers of two different tetrahedra are indicated as 1 and 2 (ref. 11)

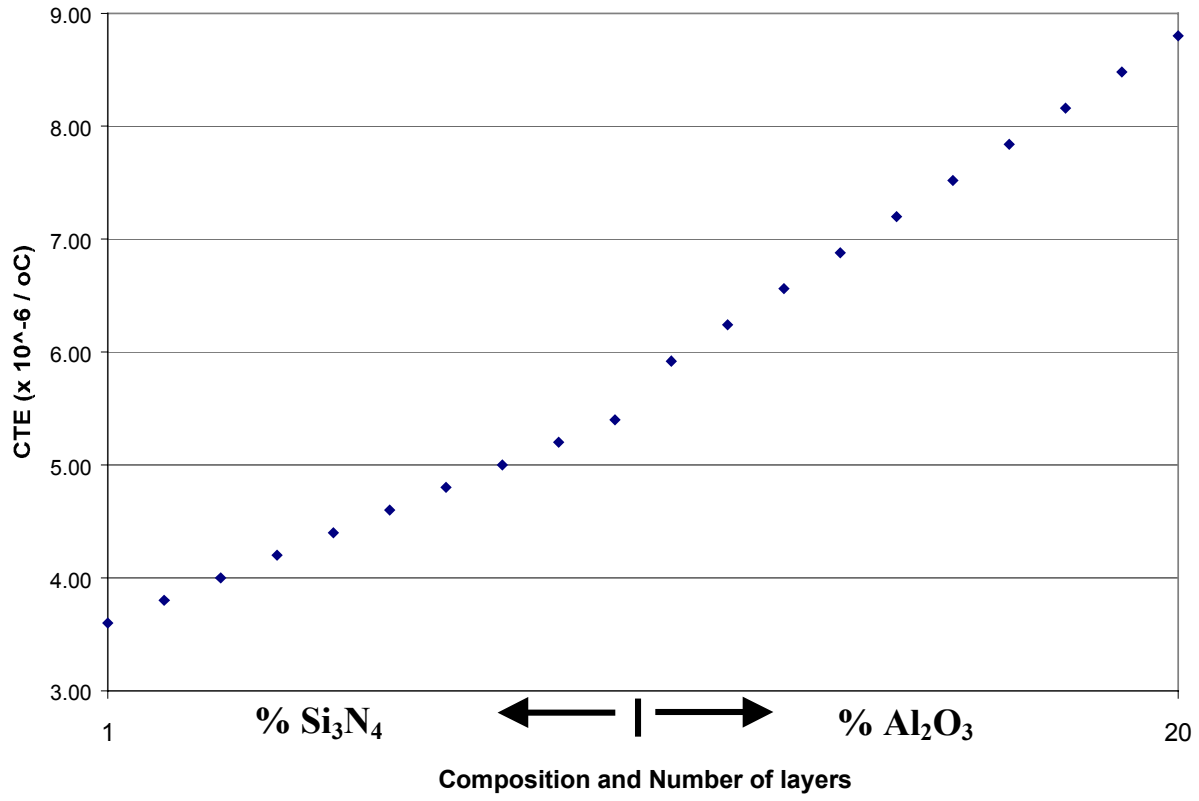


Figure 3. Calculated CTE gradient along FGM sample using the "Mixture rule"

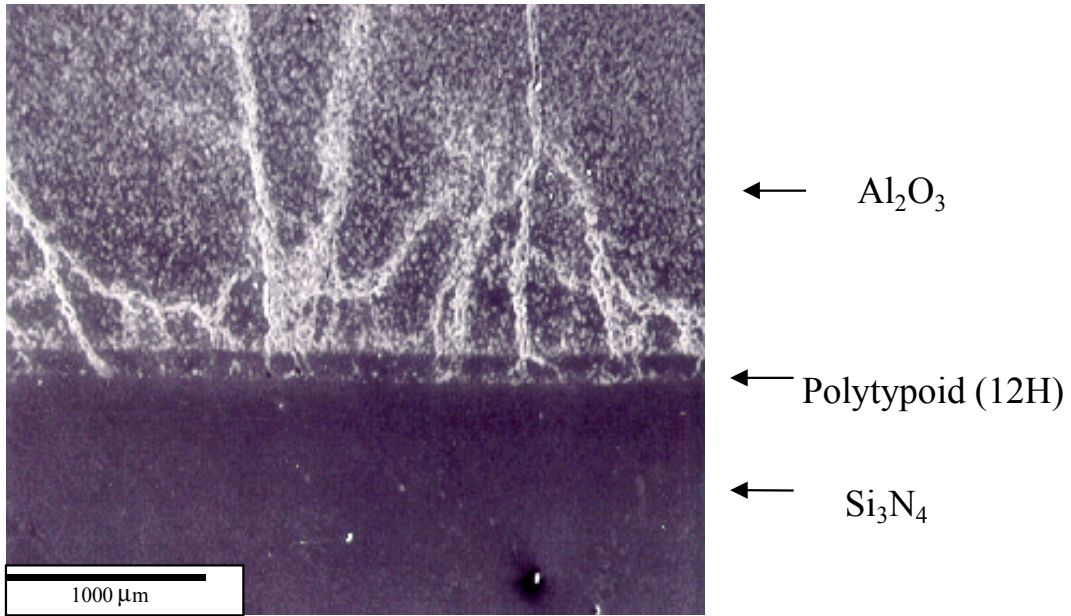


Figure 4a. Direct joining

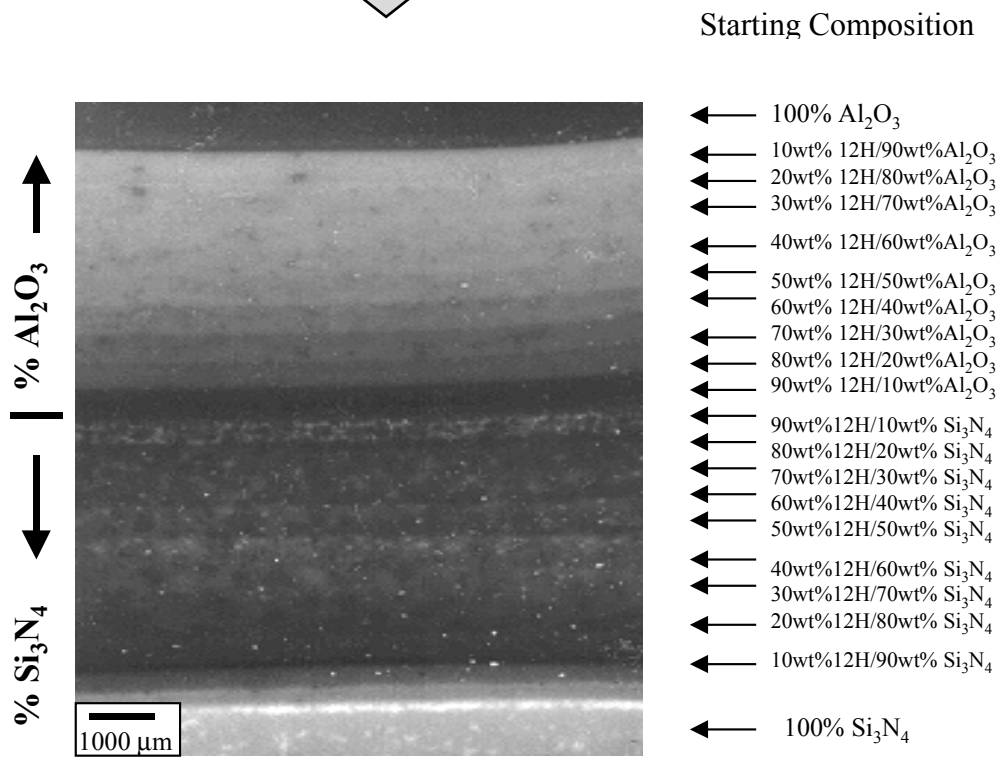
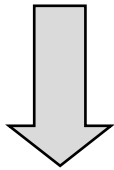


Figure 4b. FGMs

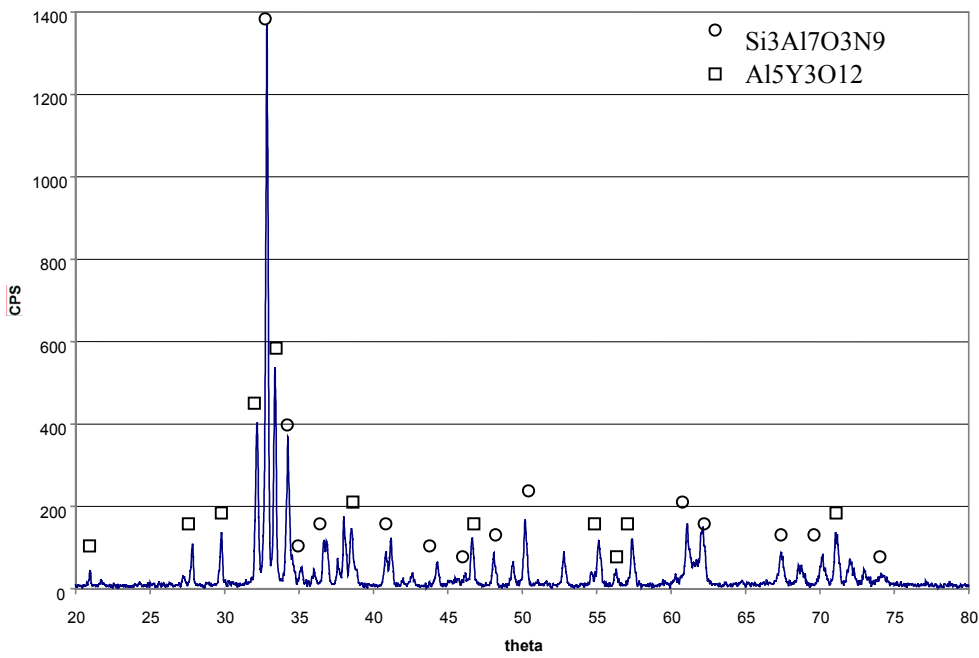


Figure 5. X-ray Diffraction pattern of polytypoid starting powder
 Note the 001 d-spacing for $\text{Si}_3\text{Al}_7\text{O}_3\text{N}_9 \sim 2.7350 \text{ \AA}$ (matches the d-spacing value for the 12H polytypoid $\sim 2.74 \text{ \AA}$)

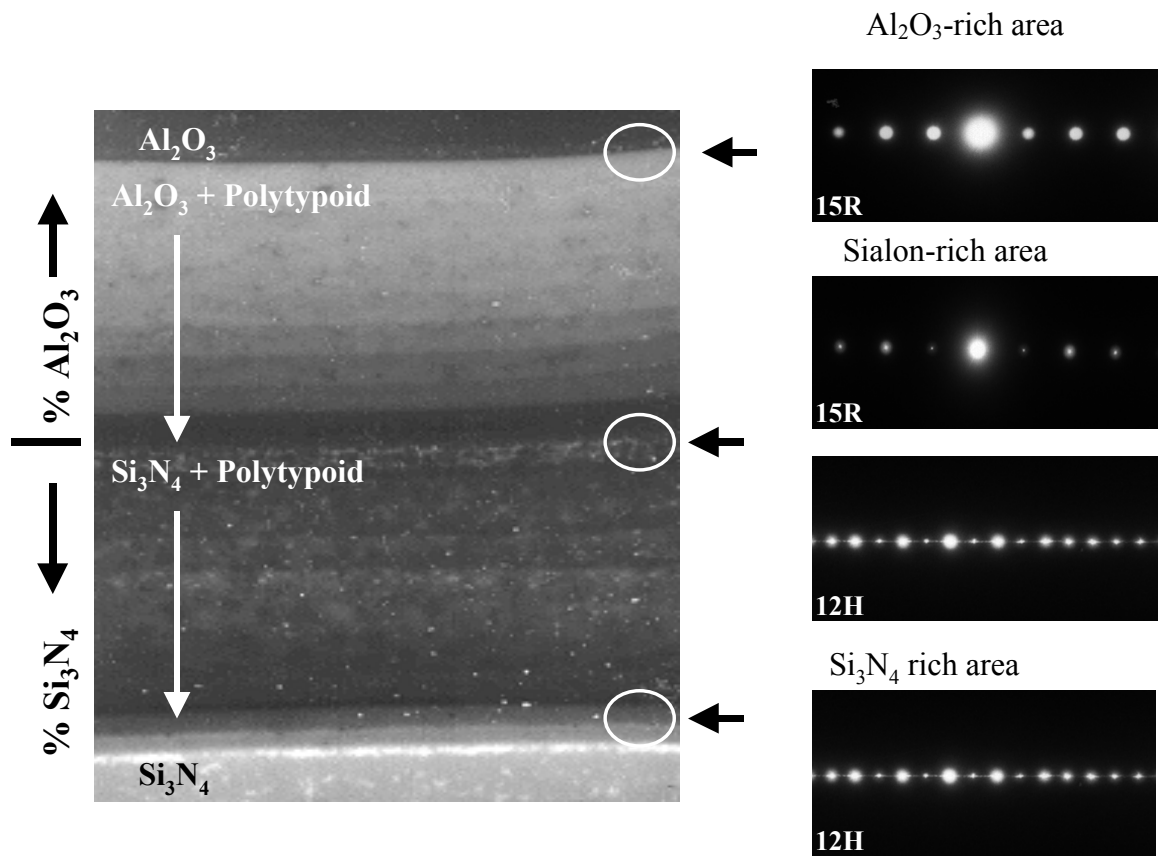


Figure 6. Diffraction patterns (RHS) of polytypoid near various interfaces (along c-axis), as shown in the light micrographs on the left side.

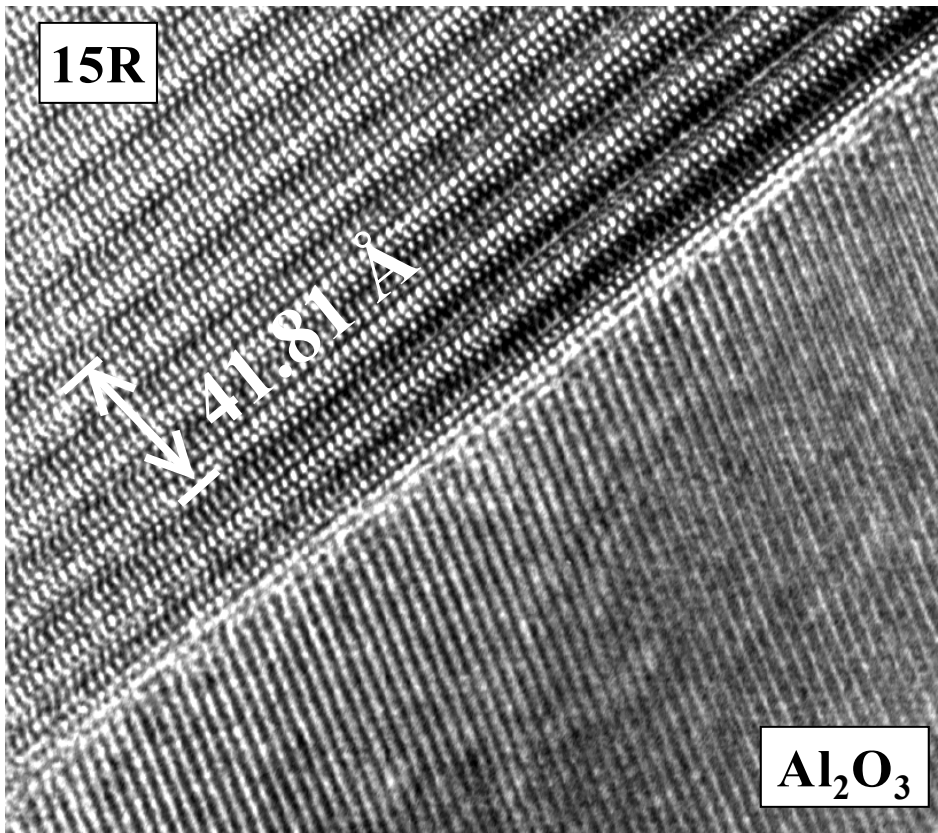
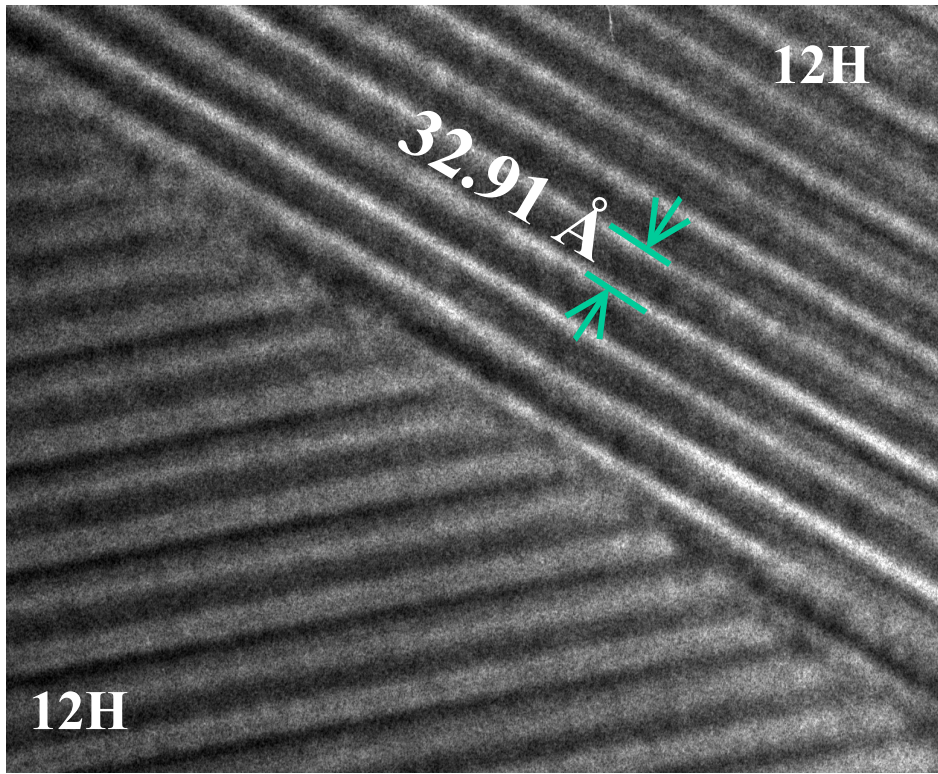


Figure 7 (a) 12H/12H (b) 15R/ Al_2O_3 (c) 15R/15R (d) 12H/ Si_3N_4 High-resolution electron microscopy images of grain boundary interfaces as indicated.

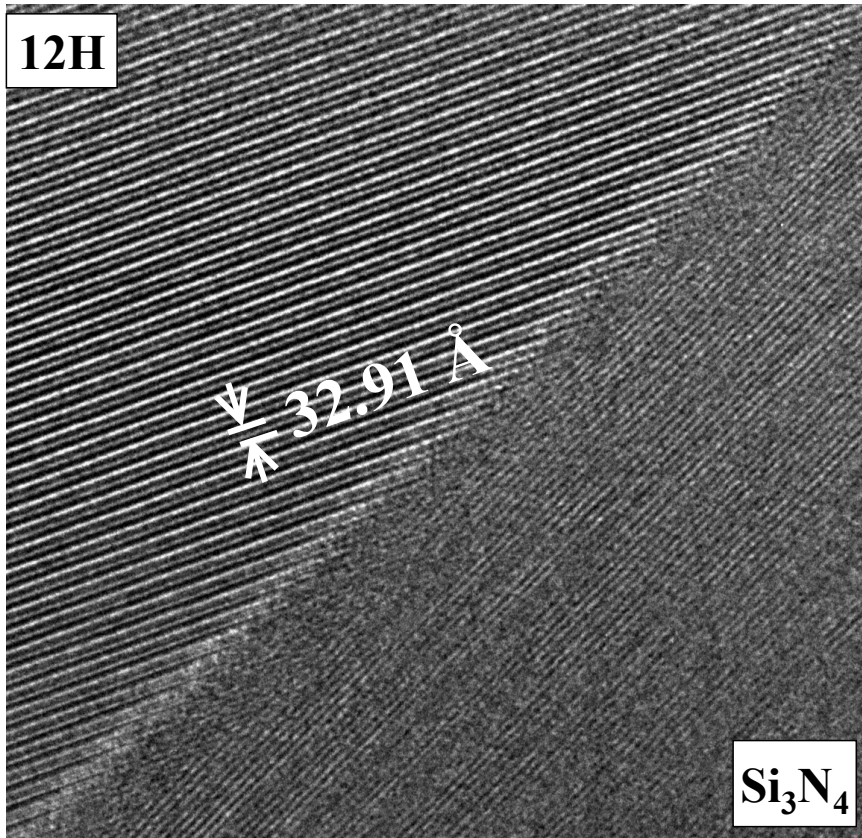
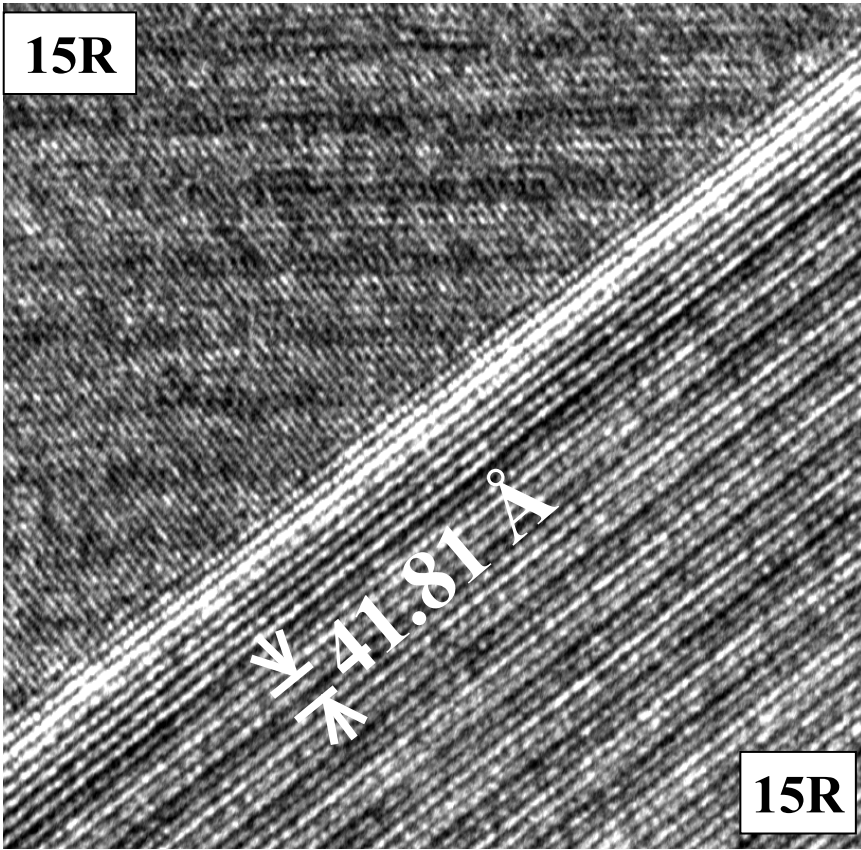


Figure 7 (c) 15R/15R (d) 12H/Si₃N₄